Supplemental Information

Optimization of Aptamer Selection on an Automated Microfluidic System with Cancer Tissues

Cheng-Sheng Lin[a], Yi-Cheng Tsai[a], Keng-Fu Hsu[d**] and Gwo-Bin Lee [a,b,c*]

[a]Department of Power Mechanical Engineering, National Tsing Hua University, Hsinchu, Taiwan.

[b]Institute of NanoEngineering and MicroSystems, National Tsing Hua University, Hsinchu, Taiwan.

[c]Institute of Biomedical Engineering, National Tsing Hua University, Hsinchu, Taiwan.

[d]Department of Obstetrics and Gynecology, National Cheng Kung University Hospital, College of Medicine, National Cheng Kung University, Tainan, Taiwan
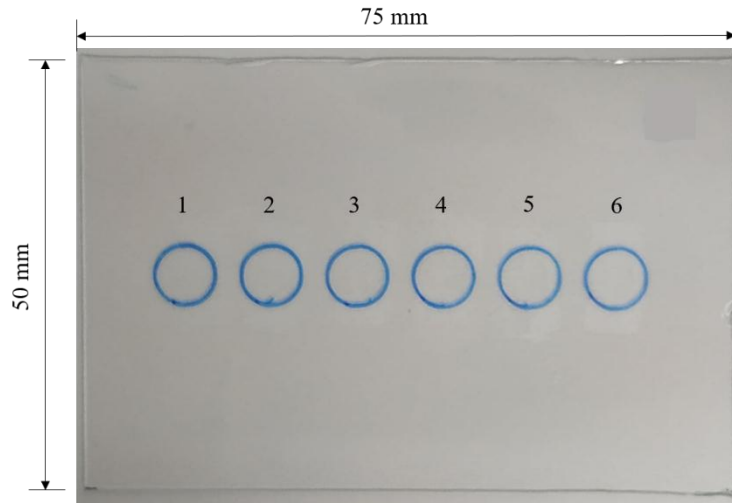
Figure S1. A photograph of the glass substrate featuring six tissue samples. Although transparent, in this image No.1 and 6 contain healthy tissues while No.2 to 5 contain cancer tissues.
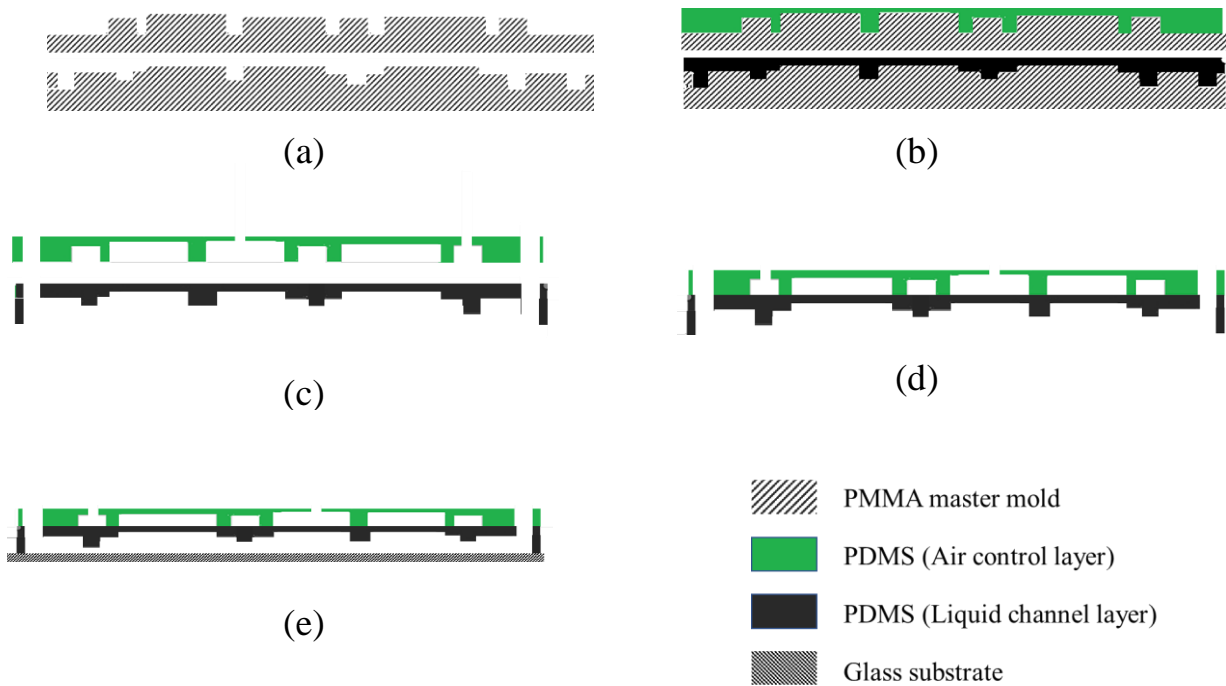

(a)

(b)

(c)

(d)

(e)

▨ PMMA master mold

■ PDMS (Air control layer)

■ PDMS (Liquid channel layer)

▨ Glass substrate

Figure S2. A flow chart of fabrication of the microfluidic chip. (a) Master molds of the microfluidic chip were fabricated by using a CNC machining process. (b) PDMS was poured onto the molds and baked at 80°C for 8 hr. (c) The PDMS replica was demolded and outlet holes were drilled. (d) The top and middle PDMS layers were bonded via oxygen plasma treatment. (e) The PDMS layers and glass substrate were bonded via oxygen plasma treatment.
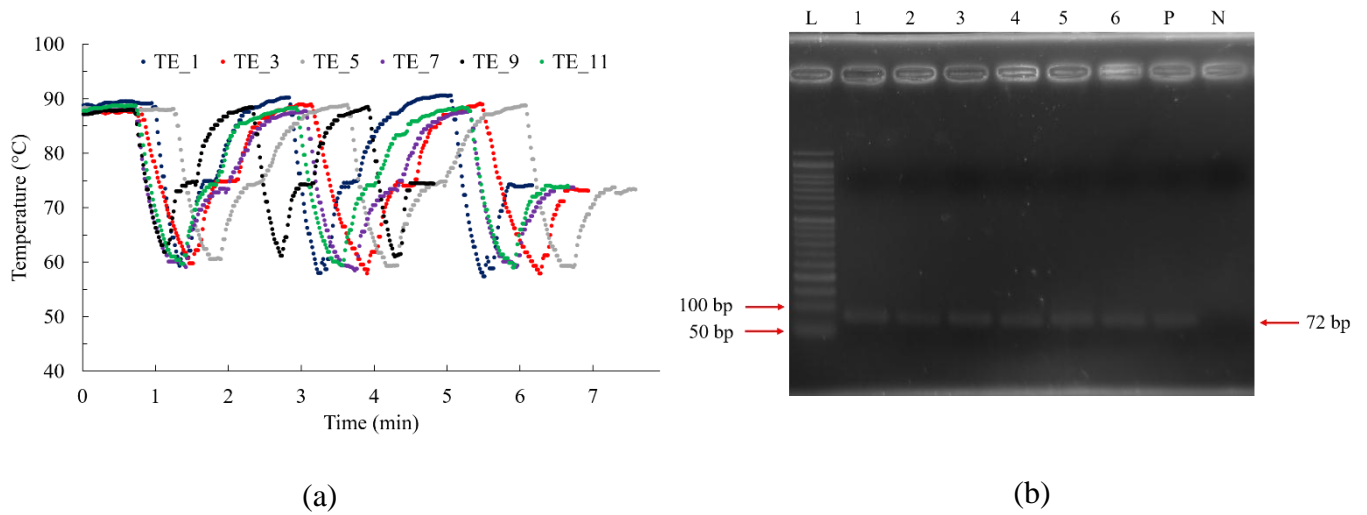
(a)

(b)

Figure S3. (a) Temperature profiles of ddH$_2$O heated by the six thermoelectric (TE) chips (to simulate PCR conditions). (b) Slab gel electropherogram depicting on-chip PCR products after 20 cycles. L: 50-bp ladders. 1~6: On-chip PCR results (TE chips 1, 3, 5, 7, 9, and 11). P: On-bench PCR (positive control). N: On-bench PCR (negative control).
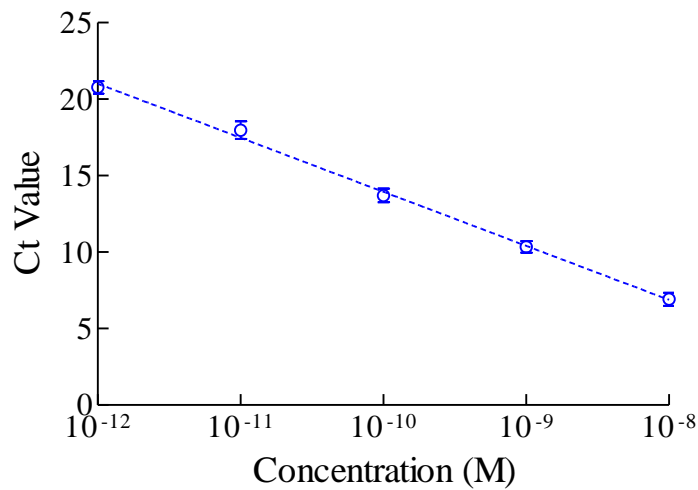

Figure S4. The relationship between Ct value and different concentrations of ssDNA library from qPCR result. The R^2 value was measured to be 0.980. Error bars represent standard deviations (n=3), and the variance was within 6%.
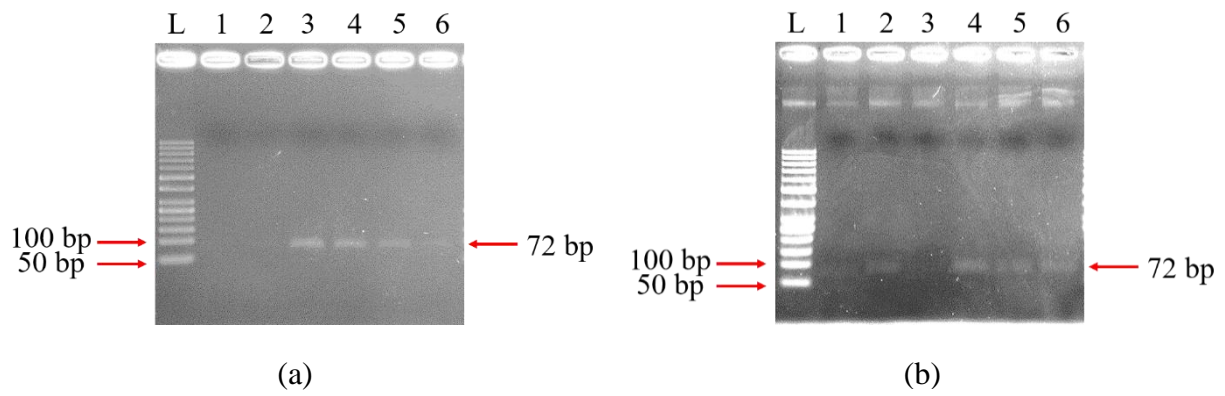
Figure S5. Slab-gel (2% agarose) electropherogram of the PCR products from optimization-tissue-SELEX under (a) a higher capture rate ion condition (Mg^{2+}, Ca^{2+}, K^+, Na^+ concentrations were 0, 50, 10, 0 mM, respectively) and (b) a lower capture rate ion condition (Mg^{2+}, Ca^{2+}, K^+, Na^+ concentrations were 0, 0, 10, 0 mM, respectively). L: 50-bp ladders. 1~6: PCR products collected from the 1st to the 6th round.
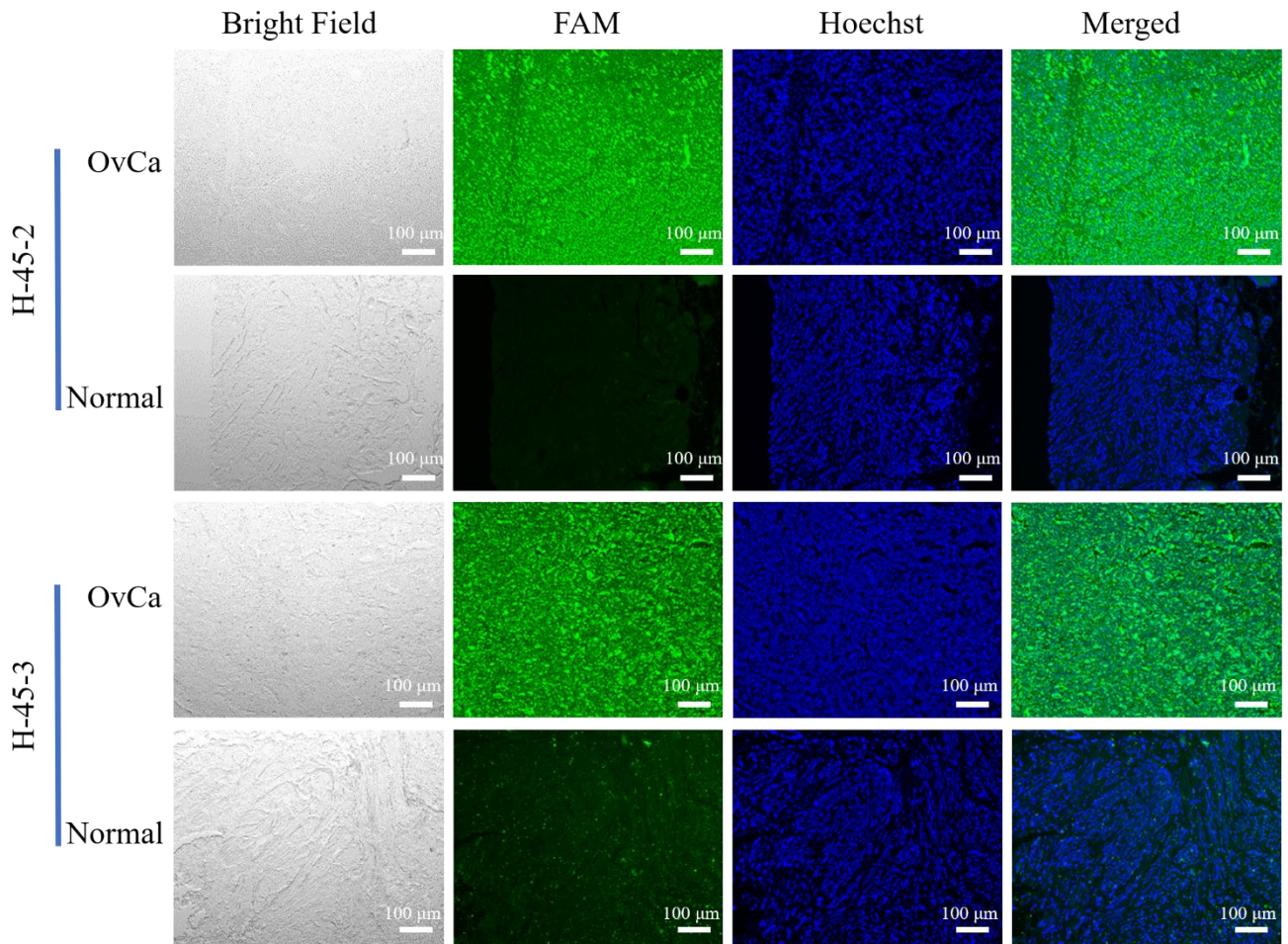
Figure S6. Fluorescent staining results of the aptamer H-45 on cancerous and healthy tissues (n=2 each). Green: FAM-labelled aptamers. Blue: Hoechst nuclear staining. Bright field images indicate the edges of the tissue samples
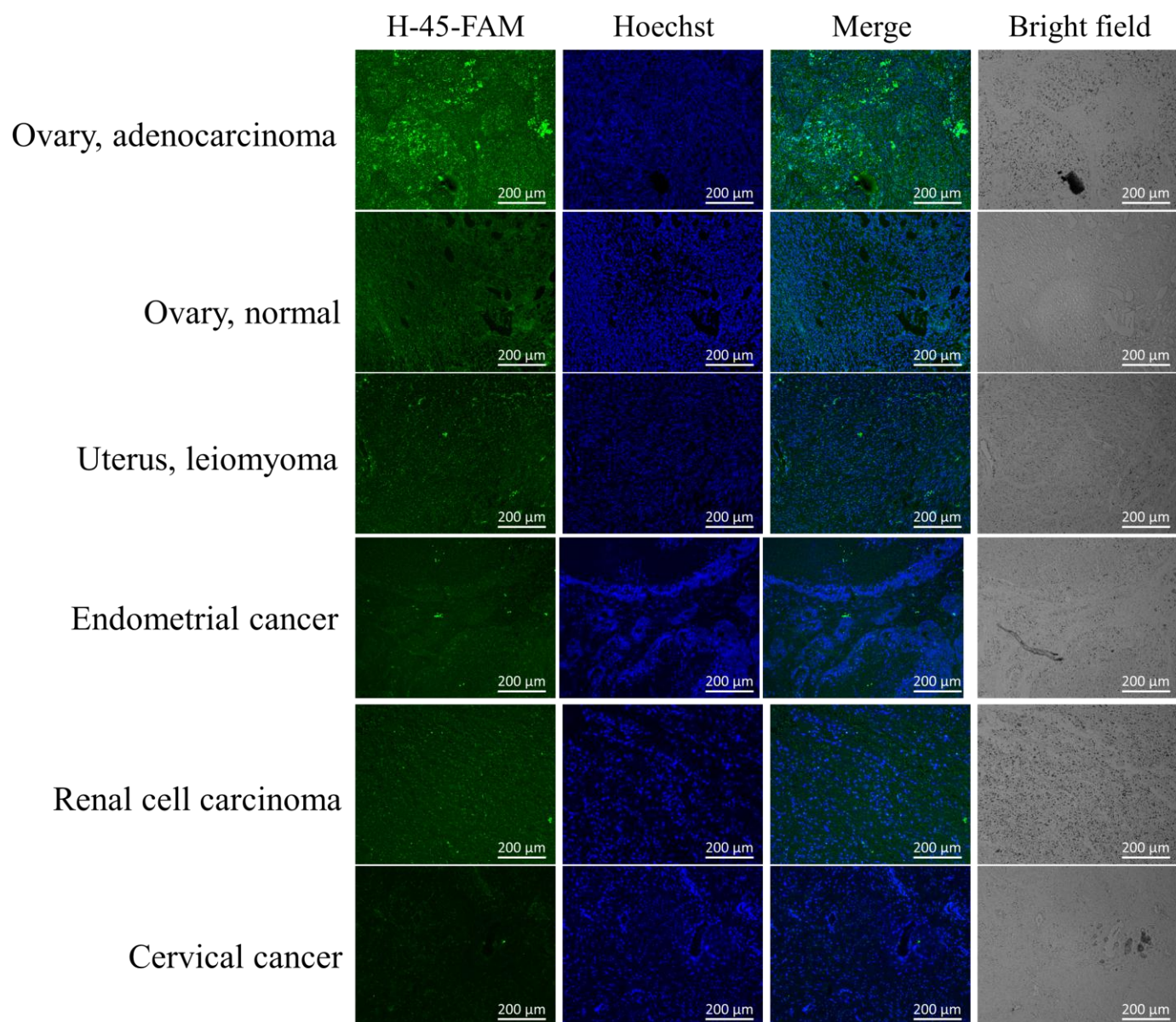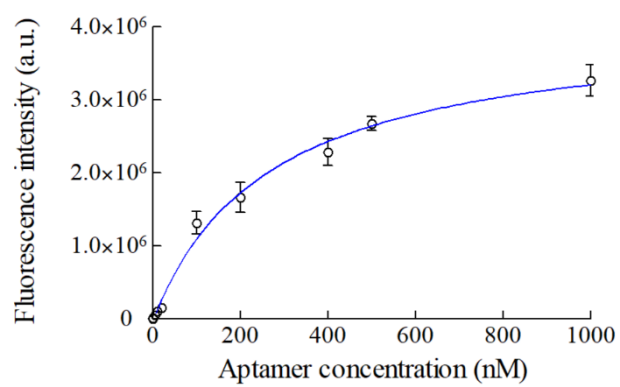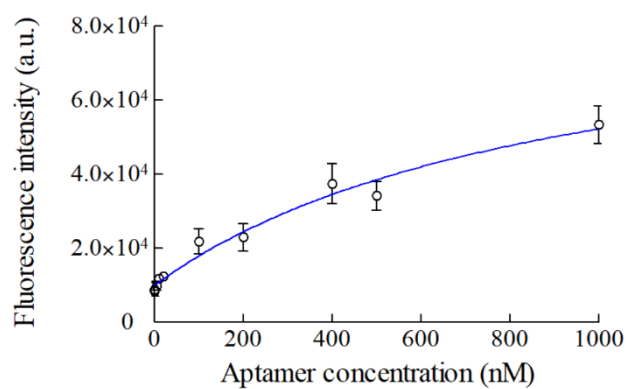
Figure S7. Fluorescent staining results of the aptamer H-45 on the clinical tissues of different cancer types. Green: FAM-labelled aptamers. Blue: Hoechst nuclear staining. Bright field images indicate the edges of the tissue samples

Figure S8. The binding affinity analysis of aptamer (a) H-45 and (b) L-25. Error bars represent standard deviations (n=3). The Kd values were measured to be 266±48 and 920±436 nM, respectively.